J. Fluid Mech. (1985), *vol.* 156, *pp.* 257–279
Printed in Great Britain

A singular-perturbation theory of the growth of a bubble cluster in a superheated liquid

By GEORGES L. CHAHINE AND HAN LIEH LIU
Tracor Hydronautics Inc., 7210 Pindell School Road, Laurel, Maryland

(Received 4 October 1983 and in revised form 5 October 1984)

The presence and behaviour of vaporous cavities are of major importance in many modern industrial applications where heat transfer, boiling or cavitation are involved. Following a sudden depressurization of a superheated fluid, the bubble growth rate controls the generated transients and heat transfer. Most existing computer modelling and prediction codes are based on individual spherical-bubble-growth studies and neglect possible interactions and collective phenomena. This paper addresses this collective behaviour using a singular-perturbation approach. The method of matched asymptotic expansions is used to describe the bubble growth, taking into account its interaction with a finite number of surrounding bubbles. A computer program is developed and the influence of the various parameters is studied numerically for the particular case of a symmetrical equal-size-bubble configuration and a thermal-boundary-layer approximation. A significant influence of these interactions on bubble growth and heat transfer is observed: compared to an isolated-bubble case, the growth rate of a bubble is reduced in the presence of other bubbles, and the temperature drop at its wall is smaller. As a result the heat loss due to bubble growth is smaller. These effects increase with the number of interacting bubbles.

1. Introduction

The presence and behaviour of vaporous cavities are of great importance in many modern industrial applications where heat transfer, boiling, or cavitation are involved. For instance, the rate of heat transfer in nucleate boiling depends essentially on the ability of the heat-transfer surface to nucleate and support the growth of vapour bubbles. The conduction of heat in the liquid is greatly affected by the absorption and release of latent heat during the phase transition at the bubble–liquid interfaces. Wave propagation in the medium is also significantly affected by bubble behaviour and volume changes. Consequently, the study of the bubble dynamics and of the two-phase medium constituted by the host liquid and bubbles of its own vapour is fundamental in the design, analysis, and application of various engineering systems.

Many modern processes deal with various fluids in conditions where both heat-transfer effects and inertia contribute in controlling the bubble behaviour. Examples of such fluids are hydrocarbons, liquid metals, cryogenic fluids, and demineralized hot water at temperatures as high as 300 °C. Heat transfer, boiling or cavitation appears with these liquids in such applications as high-speed flows of sodium-cooled fast-breeder reactors in nuclear-power engineering, circulation of cryogenic liquid in pumps in aerospace engineering, and flow of hot water in nozzles and tubes in

steam-power plants. Accidents, such as loss of vacuum insulation in cryogenic storage tanks and loss of coolant in nuclear-power plants, are sources of boiling nucleation and are of major safety concern (Plesset 1980).

The problem of the growth of an isolated spherical bubble in an unbounded fluid has been extensively studied both for cavitation problems and for heat-transfer boiling problems (see the review by Prosperetti & Plesset 1978). However, non-spherical-bubble dynamics as well as the interaction between bubbles have been given much less attention owing to the complexity of the non-spherical free-boundary-value problem. Even though it is recognized that bubbles in a boiling liquid are seldom spherical and isolated, very few studies of the subject have been made. On the other hand, many experimental and theoretical investigations exist for non-spherical-cavitation-bubble collapse (Hammitt 1980; Plesset & Prosperetti 1977; Chahine 1981*b*) and a few studies have been recently published on the inertia-controlled collapse of a multibubble system or a bubble cloud (Morch 1981; Chahine 1981*a*, 1982).

In previous work, we investigated analytically and numerically the collapse of a bubble cloud due to an increase in the ambient pressure, neglecting heat transfer (Chahine 1981*a*, 1982). A cumulative effect was shown, leading to pressures generated during the collapse significantly larger than would be computed by adding the effects of individual bubbles. This explained the observations of bent trailing edges of propellers subjected to cloud cavitation. In the work described in this paper, we extend the singular-perturbation approach earlier developed to the study of cases where heat-transfer effects cannot be neglected. We then investigate numerically the growth of a bubble cloud in a superheated fluid following a sudden depressurization. Both a general approach and a thermal-boundary-layer approximation are studied analytically, and methods of numerical solution are described. Numerical computations are then conducted only for the case of a symmetrical bubble-cloud configuration with the boundary-layer approximation and when deviations from sphericity are moderate.

2. Analytical model

2.1. *Formulation of the problem*

As a first step in studying the general problem of a bubble cloud in a flow field and near solid boundaries, let us consider a cloud of bubbles in an unbounded medium of uniform pressure P_∞ and temperature T_∞. This corresponds to the case where the size of the cloud is small compared to the flow-field characteristic lengthscale. P_∞ and T_∞ are then the local values of the pressure and the temperature in the flow field in the absence of the cloud. We further assume the liquid to be inviscid and incompressible and the flow irrotational. These assumptions are commonly accepted and are justified in cavitation and boiling heat-transfer studies except in the last phases of the bubble collapse. The neglect of the finite sound-speed effects can be unacceptable in the very early phases of the bubble growth (Baumeister & Hamill 1969). However, we will not be concerned with these early times ($t < 10^{-8}$ s), especially since numerical experiments have shown that the later history is very little influenced by the value of the initial time at which the computation is started. The bubble-cloud behaviour is of interest when the ambient pressure $P_\infty(t)$ is time dependent.

In order to determine the flow field in the bubble–liquid medium and to obtain

the motion and deformation of any bubble in the cloud one has to solve the Laplace equation for the velocity potential Φ,

$$\Delta\Phi = 0, \tag{1}$$

subjected to kinematic and dynamic conditions on the bubbles' surfaces.

The equation of a bubble surface in a coordinate system moving with velocity $\dot{b}^i$ in the direction $\boldsymbol{e}_z$, is $r = R^i(\theta, \phi, t)$. $\mathscr{C}^i$ and $\boldsymbol{n}^i$ are respectively the local curvature of the surface of bubble $B^{(i)}$ and its normal unit vector at the point $M(r, \theta, \phi)$. γ and T_R are respectively the surface tension of the liquid and its temperature at the bubble wall. P_v is the pressure of the vapour inside the bubble. The boundary conditions can then be written:

$$\nabla\Phi\cdot\boldsymbol{n}^i|_{r=R^i(\theta,\phi,t)} = [\dot{R}^i\boldsymbol{e}_r + \dot{b}^i\boldsymbol{e}_z]\boldsymbol{n}^i, \tag{2}$$

$$\rho[\dot{\Phi} - \dot{b}^i\boldsymbol{e}_z + \tfrac{1}{2}|\nabla\Phi|^2_{r=R^i(\theta,\phi,t)}] = P_\infty(t) - P^i_v(T_R) + 2\gamma^i(T_R)\mathscr{C}^i(\theta,\phi,t), \tag{3}$$

where Φ and the operator ∇ are expressed in the moving-coordinates system. Owing to the low value of the vapour density, ρ_v, the pressure of the vapour inside the bubble can be assumed to be uniform as long as the spherical symmetry is preserved. In this case, P_v is equal to the value of the equilibrium vapour pressure of the liquid at the bubble-wall temperature. We will assume that when the bubble shape deviates moderately from a sphere both the temperature along the bubble wall and the value of the vapour pressure vary accordingly. Under this assumption, the pressure P_v may be uniform inside the bubble far from the bubble surface but accommodates itself to the temperature-controlled value in the vicinity of the interface. More details on the way this happens inside the bubble are not needed here since the flow field of the vapour is of no relevance as long as the velocities are subsonic.

The value of the equilibrium vapour pressure $P_v(T_R)$ and of the surface tension $\gamma(T_R)$ constitute the coupling between the dynamic and the heat problems. To determine the temperature at the bubble wall $T_R(\theta, \phi, t)$, one needs to solve the energy equation

$$\dot{T} + \nabla\Phi\cdot\nabla T = D\cdot\Delta T, \tag{4}$$

where D is the thermal diffusivity of the liquid.

Equation (4) is subjected to a boundary condition on the bubble wall stating that the heat locally lost at any point of the interface is used to vaporize an amount of liquid determined by the local bubble-volume expansion rate. If ρ_v is the vapour density, L is the latent heat of the liquid, and K its thermal conductivity, the heat-balance equation over the bubble surface can be written in spherical coordinates:

$$K\int\int \frac{\mathrm{d}T}{\mathrm{d}n^i}\bigg|_{r=R^i(\theta,\phi,t)} R^{i2}(\theta,\phi,t)\sin\theta\,\mathrm{d}\theta\,\mathrm{d}\phi = \rho_v L\frac{\mathrm{d}}{\mathrm{d}t}\left[\int\int \frac{R^{i3}(\theta,\phi,t)}{3}\sin\theta\,\mathrm{d}\theta\,\mathrm{d}\phi\right]. \tag{5}$$

This equation is satisfied if the following elementary equilibrium equation applies locally at the bubble surface:

$$\frac{\partial T}{\partial n^i}\bigg|_{r=R^i(\theta,\phi,t)} = \frac{\rho_v L}{K}\dot{R}^i. \tag{6}$$

Equations (1)–(6) form, with the initial and at-infinity conditions (known T_∞ and $P_\infty(t)$), a complete set of equations which must be solved to determine the flow and temperature fields.

2.2. *Asymptotic approach*

The solution of the general problem as presented above is not at present conceivable. However, when the bubbles' characteristic radius r_{b_0} is small compared to the characteristic distance between two bubbles l_0 an approximate solution can be sought. For such a low-void-fraction cloud, we can assume that bubble interactions are weak enough so that, to the first order of approximation and in the absence of relative velocity with the surrounding fluid, each of the individual bubbles reacts to the local pressure variations spherically, as if isolated. Thus, to first order, after being subjected to an ambient pressure drop, the cluster behaves as a distribution of flow sources and heat sinks. Mutual bubble interactions, individual bubble motions and deformations come into play at the following orders of approximation and introduce higher-order singularities.

The solution of the problem is sought in terms of matched asymptotic expansions in powers of ϵ, the ratio between r_{b_0} and l_0. Two regions of the fluid are defined for each individual bubble of the cloud. The 'outer region' is that considered when the reference length is chosen to be l_0. The corresponding 'outer problem' is concerned with the macro-behaviour of the cloud, and the bubbles appear in it only as singularities. The 'inner region' is that considered when the lengthscale is r_{b_0}. The solution of the corresponding 'inner problem' applies to the microscale of the cloud, i.e. to the vicinity of an individual bubble of centre B_i. The presence of the other bubbles, all considered to be at infinity for the 'inner problem', is sensed, at each order of approximation, by the asymptotic behaviour of the outer solution in the vicinity of B_i. Thus, to each order of approximation the 'inner problem' reduces to the study of an isolated bubble with conditions imposed at infinity determined at the preceding orders. These conditions are obtained as the expansions of the preceding orders' 'outer solution' near the bubble singularity and by application of the matching principle. The process is started by the first-order approximation, whose solution is known since all bubbles then behave as if isolated.

2.3. *Normalizations*

In order to generate asymptotic expansions (and thus to compare orders of magnitudes) an accurate choice of characteristic scale variables is fundamental. For the lengthscales the choice is immediate: r_{b_0} in the inner problem, l_0 in the outer. However, the relationship between r_{b_0} and the characteristic initial bubble radius R_0 is not obvious. Indeed, while, in the case of bubble collapse, the bubble radius stays of order R_0 in the mathematical sense ($R(\epsilon) = O(R_0)$ if there exists a constant λ independent of ϵ such that $|R| < \lambda |R_0|$), this is not the case for the bubble-cloud growth studied here. Therefore r_{b_0} is chosen arbitrarily to be much larger than R_0 but such that the inequality

$$r_{b_0}/l_0 = \epsilon \ll 1 \tag{7}$$

is valid. Consequently, the results of the computations will be valid only as long as the radius of any bubble in the cloud does not greatly exceed r_{b_0}.

Concerning the timescale, the choice is simple once r_{b_0} is known. In the case of a significant pressure drop, as for the problem of sudden depressurization in a loss-of-coolant accident, this timescale is related to the pressure drop ΔP, through

$$\tau_0 = r_{b_0}\left(\frac{\rho}{\Delta P}\right)^{\frac{1}{2}}. \tag{8}$$

ΔP could also be the order of magnitude of the imposed pressure fluctuations when $P_\infty(t)$ is a prescribed function of time.

As mentioned earlier, in both 'inner' and 'outer' regions, the flow in the first approximation is that due to a distribution of dynamic sources and heat sinks. The characteristic strength of the dynamic sources is $q_0 = r_{b_0}^3/\tau_0$, and, depending on whether one considers the 'inner' or the 'outer' problem, the resulting velocity potential Φ has the scales:

$$\Phi_0^{\text{in}} = \frac{r_{b_0}^2}{\tau_0}, \quad \Phi_0^{\text{out}} = \frac{r_{b_0}^3}{l_0 \tau_0}. \tag{9}$$

Since the maximum temperature drop occurs near the bubble wall, and since a lower bound for this temperature is the boiling temperature of the liquid T_b, at the imposed ambient pressure P_∞, the temperature departure from T_∞ is scaled with the amount of superheat $(T_\infty - T_b)$.

With these characteristic scales, non-dimensional variables, all of order unity, are introduced through the following definitions, where bars denote outer non-dimensional variables and tildes inner ones:

$$\left.\begin{aligned} &\tilde{r} = \frac{r}{r_{b_0}}; \quad \bar{r} = \frac{r}{l_0}; \quad \bar{l}^{ij}(t) = \frac{l^{ij}(t)}{l_0}; \quad \tilde{b}(t) = \frac{\dot{b}\tau_0}{r_{b_0}}; \quad \tilde{t} = \bar{t} = \frac{t}{\tau_0}; \\ &\tilde{T} = \bar{T} = \frac{T}{T_\infty - T_b}; \quad \tilde{p}(t) = \bar{p}(t) = \frac{p(t)}{\Delta P}; \quad \tilde{\Phi}(t) = \frac{\Phi^{\text{in}}(t)}{\Phi_0^{\text{in}}}; \quad \bar{\Phi}(t) = \frac{\Phi^{\text{out}}(t)}{\Phi_0^{\text{out}}}. \end{aligned}\right\} \tag{10}$$

Each of the unknowns X is then expanded in power series of ϵ as follows:

$$X = X_0 + \epsilon X_1 + \epsilon^2 X_2 + \epsilon^3 X_3 + O(\epsilon^3). \tag{11}$$

3. Singular perturbation approach

3.1. *First order of approximations* (ϵ^0)

When ϵ is zero, the distance between bubbles is infinity, interactions vanish, and, in the absence of a slip velocity between the test bubble and the surrounding fluid, the only boundary condition at infinity is the imposed ambient pressure variation $P_\infty(t)$. The 'inner problem' is therefore spherically symmetrical and its solution is given by the well-known Rayleigh–Plesset equation. This can be written with the superscript (i) omitted for convenience:

$$\tilde{a}_0 \ddot{\tilde{a}}_0 + \tfrac{3}{2}\dot{\tilde{a}}_0^2 = -\tilde{P}_\infty(t) + \pi_0(t) - \frac{2W_e^{-1}}{\tilde{a}_0}\tilde{\gamma}(t) - \mathscr{P}. \tag{12}$$

The non-dimensional parameters are defined by the relations:

$$\left.\begin{aligned} &\tilde{P}_\infty(t) = \frac{P_\infty(t) - P_\infty(0)}{\Delta P}, \quad \mathscr{P} = \frac{P_\infty(0) - P_v(0)}{\Delta P}, \\ &\pi_0(t) = \frac{p_v(t) - p_v(0)}{\Delta P}, \quad W_e^{-1} = \frac{\gamma(0)}{r_{b_0}\Delta P}, \quad \tilde{\gamma}(t) = \frac{\gamma(t)}{\gamma(0)}. \end{aligned}\right\} \tag{13}$$

$\gamma(t)$ and $p_v(t)$ are, respectively, the surface-tension coefficient and the liquid vapour pressure at the bubble-wall temperature at time t. The initial equilibrium condition at the bubble interface is

$$\mathscr{P} + \frac{2W_e^{-1}}{R_0} = 0. \tag{14}$$

For a given $P_\infty(t)$, (12) can be solved for the variations of the bubble radius, $\tilde{a}_0^i(t)$. This allows the subsequent determination of the higher-order approximations of the bubble radius.

When the temperature at the surface of the bubble departs significantly from the ambient temperature, it is necessary to couple (12) with the energy equation to account for the dependence of p_v and γ on temperature. At this order, the problem is spherically symmetrical, and the energy equation (4) reduces to the following non-dimensional equation:

$$\frac{\partial \tilde{T}_0}{\partial \tilde{t}} - \frac{\tilde{a}_0^2 \dot{\tilde{a}}_0}{\tilde{r}^2} \frac{\partial \tilde{T}_0}{\partial \tilde{r}} = P_e^{-1} \frac{1}{\tilde{r}^2} \frac{\partial}{\partial \tilde{r}} \left(\tilde{r}^2 \frac{\partial \tilde{T}_0}{\partial \tilde{r}} \right), \tag{15}$$

where the Péclet number P_e is the ratio of the thermal diffusion time $r_{b_0}^2/D$ to the bubble characteristic time τ_0,

$$P_e = r_{b_0}^2 / D\tau_0. \tag{16}$$

The heat balance on the bubble–liquid interface reduces at this order of approximation to the following normalized equation:

$$\frac{\partial \tilde{T}_0}{\partial \tilde{r}} = \frac{\rho_v L r_{b_0}^2}{K \tau_0 (T_\infty - T_b)} \dot{\tilde{a}}_0 = \mathscr{A} \dot{\tilde{a}}_0. \tag{17}$$

3.2. *Interactions*

3.2.1. *Order* ϵ

In the asymptotic theory presented here, the local pressures and temperatures driving the growth of any bubble $B^{(i)}$ are a perturbation of the imposed far-field pressure $P_\infty(t)$ and temperature T_∞. Since these perturbations are due to the presence of the other bubbles in the flow field, the leading terms can be obtained directly once the first-order behaviour of all the bubbles in the cloud is determined. For instance, once (12), (15), and (17) are solved, the variation with time of the radius, $a_0^j(t)$, of any cavity in the cloud can be determined. This allows the determination of the intensity of all sources $q_0^j(t)$:

$$\tilde{q}_0^j(t) = \tilde{a}_0^{j^2} \dot{\tilde{a}}_0^j. \tag{18}$$

Consequently, the resultant 'outer' potential flow is determined to this order by

$$\bar{\Phi}_0(M,t) = \sum_{j=1}^{N} \frac{\tilde{q}_0^j(t)}{|\overline{MB^j}|}, \tag{19}$$

where M is a field point, and B^j the centre of the bubble $B^{(j)}$, and also the location of the source (j). The asymptotic expansions of $\bar{\Phi}_0(M,t)$, when the normalized distance $|\overline{MB^i}| = \epsilon \tilde{r}^i$ goes to zero, contain additional terms other than the leading source term, $\tilde{q}_0^i/\tilde{r}^i$, corresponding to the order-zero 'inner' potential flow,

$$\tilde{\Phi}_0^i = \tilde{q}_0^i(t)/\tilde{r}^i. \tag{20}$$

These terms express the interactions and are responsible for the flow and bubble-shape corrections. For instance, by application of the matching principle (n–m rule, Van Dyke 1964), the order-ϵ term will determine the boundary condition at infinity for the order-ϵ 'inner' velocity potential, i.e.

$$\lim_{\tilde{r}^i \to \infty} \tilde{\Phi}_1^i = \sum_{j \neq i} \left(\frac{l_0}{l_0^{ij}} \right) \tilde{q}_0^j, \tag{21}$$

where l_0^{ij} is the initial distance between the two cavities' centres B^i and B^j.

In addition to the at-infinity boundary condition (21) the first correction, $\tilde{\Phi}_1^i$, of the undisturbed potential flow $\tilde{\Phi}_0^i$ has to satisfy the Laplace equation (1), as well as boundary conditions on the surface of the bubble $B^{(i)}$. These are the contributions to order ϵ of the expansions in powers of ϵ of conditions (2) and (3) made dimensionless. Similarly, the first correction, T_1, of T_0 has to satisfy the equations derived from (4) and (6).

Owing to condition (21) the dynamic problem remains spherical. To this order the effect of the other bubbles does not introduce any asymmetries, and only changes the level of the velocity potential. Therefore the correction at this order stems from a modification in the 'inner' problem of the pressure imposed at infinity by the time derivative of the added at-infinity velocity potential (21). As a result, the solution of the dynamic problem at order ϵ is again given by a source term which corrects the leading term $\tilde{\Phi}_0^i$. This solution can be written:

$$\tilde{\Phi}_1^i = \frac{\tilde{q}_1^i(t)}{\tilde{r}} + \sum_{j \neq i} \left(\frac{l_0}{l_0^{ij}}\right) \tilde{q}_0^j(t), \tag{22}$$

where the source intensity, $\tilde{q}_1^i$, is given by

$$\tilde{q}_1^i = \tilde{a}_0^{i^2} \dot{\tilde{a}}_1^i + 2\tilde{a}_0^i \dot{\tilde{a}}_0^i \tilde{a}_1^i. \tag{23}$$

In order to satisfy the boundary conditions at the bubble surface, the first correction, $\tilde{a}_1^i$, of the bubble radius has to satisfy the following differential equation, where the superscript i has been omitted:

$$\tilde{a}_0 \ddot{\tilde{a}}_1 + 3\dot{\tilde{a}}_0 \dot{\tilde{a}}_1 + \tilde{a}_1(\ddot{\tilde{a}}_0 - 2W_e^{-1}\tilde{a}_0^{-2}) = -\sum_{j \neq i} \left(\frac{l_0}{l_0^{ij}}\right) \tilde{q}_0^j + \pi_1(t). \tag{24}$$

$\pi_1(t)$ is a correction of $\pi_0(t)$ and expresses the second approximation of the value of the vapour pressure at the bubble wall. Using the expansions of the temperature in powers of ϵ as in (11), $\pi_0(t)$ and $\pi_1(t)$ can be expressed as

$$\pi_0(t) = \frac{p_v(T_0(a_0, t)) - p_v(T_\infty)}{\Delta P}, \tag{25}$$

$$\pi_1(t) = \frac{p_v[T_1(a_0, t)] + a_1 \dfrac{\partial T_0}{\partial r}(a_0, t) \dfrac{\mathrm{d}p_v}{\mathrm{d}T}[T_0(a_0, t)]}{\Delta P}. \tag{26}$$

For the study of the heat problem it is useful to introduce the following variable (again omitting the superscripts i):

$$y = \tfrac{1}{3}[\tilde{r}^3 - \tilde{R}^3(\theta, t)], \tag{27}$$

by analogy with the spherical-bubble case (Prosperetti & Plesset 1978). With this variable change, the normalized energy equation can be written:

$$\dot{\tilde{T}} + \frac{\partial \tilde{T}}{\partial y}\left[\tilde{r}^2 \frac{\partial \tilde{\Phi}}{\partial r} - \tilde{R}^2 \dot{\tilde{R}}\right]$$
$$= P_e^{-1}\left\{\frac{\partial}{\partial y}\left(\tilde{r}^4 \frac{\partial \tilde{T}}{\partial y}\right) + \frac{1}{\tilde{r}^2 \sin\theta}\left[\frac{\partial}{\partial \theta}\left(\sin\theta \frac{\partial \tilde{T}}{\partial \theta}\right) - \frac{\partial}{\partial \theta}\left(\tilde{R}^2 \frac{\partial \tilde{R}}{\partial \theta} \sin\theta \frac{\partial \tilde{T}}{\partial y}\right)\right]\right\} + O(\epsilon^3). \tag{28}$$

After replacing $\tilde{r}$ by its value derived from (27), and accounting for the expansions of $R(\theta, t)$, we obtain, at the orders ϵ^0 and ϵ, the relations

$$\dot{\tilde{T}}_0 - P_e^{-1} \frac{\partial}{\partial y}\left(\eta^4 \frac{\partial \tilde{T}_0}{\partial y}\right) = 0, \tag{29}$$

and
$$\tilde{T}_1 - P_e^{-1}\frac{\partial}{\partial y}\left(\eta^4\frac{\partial \tilde{T}_1}{\partial y}\right) = P_e^{-1}\frac{\partial}{\partial y}\left(4\eta\tilde{a}_1\tilde{a}_0^2\frac{\partial \tilde{T}_0}{\partial y}\right), \tag{30}$$

where
$$\eta = (\tilde{a}_0^3 + 3y)^{\frac{1}{3}}. \tag{31}$$

Similarly, the heat-balance condition on the bubble wall becomes at order ϵ^0 and ϵ:
$$\tilde{a}_0^2\frac{\partial \tilde{T}_0}{\partial y}\bigg|_{y=0} = \mathscr{A}\dot{\tilde{a}}_0, \tag{32}$$

and
$$\tilde{a}_0^2\left(\frac{\partial \tilde{T}_1}{\partial y} + 2\frac{\tilde{a}_1}{\tilde{a}_0}\frac{\partial \tilde{T}_0}{\partial y}\right)_{y=0} = \mathscr{A}\dot{\tilde{a}}_1. \tag{33}$$

3.2.2. *Higher orders*

Continuing the same procedure as in the preceding section, one can derive the successive equations for the flow field, the temperature field and the bubble motion. The solution of the problem is made easier by the use of series expansions of the velocity potential in spherical harmonics, and of the bubble-surface equation and the temperature field in Legendre polynomials, $P_n(\cos\theta)$. The boundary condition at infinity for any particular 'inner' problem (i), obtained by expanding the expression of $\bar{\Phi}$ near B^i (Chahine & Bovis 1983; Chahine 1982) can then be shown to be up to order ϵ^3:

$$\lim_{\tilde{r}\to\infty}\tilde{\Phi}^i(M,t) = \sum_{i\neq j}\{-\epsilon\lambda_{ij}\tilde{q}_0^j - \epsilon^2(\lambda_{ij}^2\tilde{q}_0^j\tilde{r}\cos\theta^{ij} + \lambda_{ij}\tilde{q}_1^j) - \epsilon^3[\lambda_{ij}^3\tilde{q}_0^j\tilde{r}^2P_2(\cos\theta^{ij}) + \lambda_{ij}^2\tilde{q}_1^j\tilde{r}\cos\theta^{ij} + \lambda_{ij}\tilde{q}_2^j] + \ldots\}. \tag{34}$$

$\tilde{q}_n^j$ is the correction at order ϵ^n of $\tilde{q}_0^j$, the strength of the source representing the first-approximation spherical volume change of the bubble $B^{(j)}$, and
$$\lambda_{ij} = (l_0/l_0^{ij}). \tag{35}$$

The superscript j denotes quantities corresponding to the other bubbles, $B^{(j)}$, and θ^{ij} is the angle MB^iB^j between B^i, B^j, and a field point in the fluid M (see figure 1).

Expressed in physical terms (velocities, pressures) the boundary condition (34) indicates that the order-ϵ correction to the non-perturbed spherical flow field around the test bubble is a spherical modification of the collapse driving pressure. This introduces, as we have seen in the preceding section, a spherical correction $\tilde{a}_1^i(t)$ to the radius variations $\tilde{a}_0^i(t)$. At the following order ϵ^2 a second correction of the at-infinity uniform pressure appears, and a uniform velocity field expressing a slip velocity between the bubble and the surrounding fluid is to be added. Going through the expansions of the boundary conditions at the bubble surface, one can show that this induces a spherical correction, $a_2^i(t)$, of $a_0^i(t)$, and a non-spherical correction $f_2^i(t)\cos\theta^{ig}$ (Chahine & Bovis 1983; Chahine 1982). θ^{ig} is an angle which can be compounded from all the θ^{ij}'s (see §3.3). Things become more complex at the order of expansion ϵ^3 where, in addition to the uniform pressure and velocity corrections, a velocity gradient generated by the flow field associated with the motion of all the other bubbles, is to be accounted for to generate a non-spherical correction of form $P_2(\cos\theta^{ig})$.

Following from the above remarks on the at-infinity boundary condition, one can

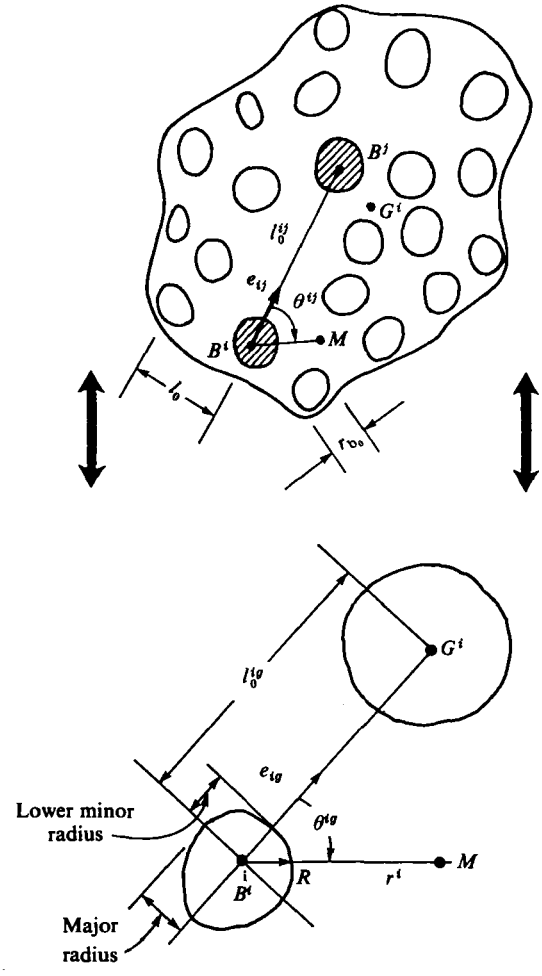

FIGURE 1. Multibubble interaction equivalence concept.

show that the equation of the surface of the bubble $B^{(i)}$ and the temperature can be written as:

$$\tilde{R}^i(\theta^{ig},t) = \tilde{a}_0^i(t)+\epsilon\tilde{a}_1^i(t)+\epsilon^2[\tilde{a}_2^i(t)+\tilde{f}_2^i(t)\cos\theta^{ig}] + \epsilon^3[\tilde{a}_3^i(t)+\tilde{f}_3^i(t)\cos\theta^{ig}+\tilde{g}_3^i(t)\,P_2(\cos\theta^{ig})]+o(\epsilon^3), \quad (36)$$

$$T(r,\theta^{ig},t) = T_0(r,t)+\epsilon T_1(r,t)+\epsilon^2[T_{20}(r,t)+T_{21}(r,t)\cos\theta^{ig}] + \epsilon^3[T_{30}(r,t)+T_{31}(r,t)\cos\theta^{ig}+T_{32}(r,t)\,P_2(\cos\theta^{ig})]+o(\epsilon^3), \quad (37)$$

provided that the initial bubble shape is spherical (Chahine 1982; Chahine & Liu 1983). Therefore, up to the order ϵ^3 each inner problem is axisymmetric, and the axis of symmetry for every bubble is in the direction, B^iG, of its motion towards the bubble-cloud 'centre' (see §3.3).

We introduce $\tilde{d}_n$ defined as the sum of the deformation rate of form $\cos\theta$, $\tilde{f}_n$, and of the origin of axis translation velocity, $\tilde{b}_n$:

$$\tilde{d}_n = \tilde{f}_n+\tilde{b}_n. \quad (38)$$

One then obtains the following differential equations for the order-ϵ^2 radius components, and $\dot{d}_2$:

$$\tilde{a}_0\ddot{\tilde{a}}_2^2+3\dot{\tilde{a}}_0\dot{\tilde{a}}_2+\tilde{a}_2(\ddot{\tilde{a}}_0-2W_e^{-1}\tilde{a}_0^{-2})=-\tfrac{3}{2}\dot{\tilde{a}}_1^2-\tilde{a}_1\ddot{\tilde{a}}_1-2W_e^{-1}\tilde{a}_1^2\tilde{a}_0^{-3}+\pi_2(t)-\sum_{i\neq j}\lambda_{ij}\tilde{q}_1^j, \quad (39)$$

$$\tilde{a}_0\ddot{\tilde{d}}_2+3\dot{\tilde{a}}_0\dot{\tilde{d}}_2=\pi_{21}(t)-3\sum_{i\neq j}\lambda_{ij}^2(\dot{\tilde{a}}_0\tilde{q}_0^j+\tilde{a}_0\dot{\tilde{q}}_0^j)\frac{\cos\theta^{ij}}{\cos\theta^{ig}}. \quad (40)$$

In the above equations, the superscript i has been omitted, and $\tilde{a}_0(t)$ and $\tilde{a}_1(t)$ are obtained at the preceding orders by solving the differential equations (12) and (24). $\pi_{nm}(t)$ are higher-order approximations of the non-dimensional difference between the vapour pressure at any time and its initial value. The indices n, m correspond to those used in the expansions of the temperature, (37).

The energy equations at order ϵ^2 can be written using

$$\eta=(\tilde{a}_0^3+3y)^{\frac{1}{3}}, \quad (41)$$

$$\dot{\tilde{T}}_{20}-P_e^{-1}\left(\eta^4\frac{\partial\tilde{T}_0}{\partial y}\right)=P_e^{-1}\frac{\partial}{\partial y}\left[(4\tilde{a}_0\tilde{a}_1^2\eta+4\tilde{a}_0^2\tilde{a}_2\eta+2a_0^4a_1^2\eta^{-2})\frac{\partial\tilde{T}_0}{\partial y}+4\tilde{a}_0^2\tilde{a}_1\eta\frac{\partial\tilde{T}_1}{\partial y}\right], \quad (42)$$

$$\begin{aligned}\dot{\tilde{T}}_{21}-P_e^{-1}\left[\frac{\partial}{\partial y}\left(\eta^4\frac{\partial\tilde{T}_{21}}{\partial y}\right)-2\eta^{-2}\tilde{T}_{21}\right]&=\left(\frac{2h_2}{\eta}+2\dot{\tilde{a}}_0\tilde{a}_0\tilde{f}_2+\tilde{a}_0^2\dot{\tilde{f}}_2+\sum_{i\neq j}\lambda_{ij}^2\tilde{q}_0^j\frac{\cos\theta^{ij}}{\cos\theta^{ig}}\eta^2\right)\frac{\partial\tilde{T}_0}{\partial y}\\&\quad+P_e^{-1}\left[2\eta^{-2}\tilde{a}_0^2\tilde{f}_2\frac{\partial\tilde{T}_0}{\partial y}+\frac{\partial}{\partial y}\left(4\eta\tilde{f}_2\tilde{a}_0^2\frac{\partial T_0}{\partial y}\right)\right]. \quad (43)\end{aligned}$$

The corresponding conditions of heat balance on the bubble wall are

$$\tilde{a}_0^2\left[\frac{\partial\tilde{T}_{20}}{\partial y}+\frac{2\tilde{a}_1}{\tilde{a}_0}\frac{\partial\tilde{T}_1}{\partial y}+2\left(\frac{\tilde{a}_2}{\tilde{a}_0}+\frac{\tilde{a}_1^2}{\tilde{a}_0^2}\right)\frac{\partial\tilde{T}_0}{\partial y}\right]_{y=0}=\mathscr{A}\dot{\tilde{a}}_2, \quad (44)$$

$$\tilde{a}_0^2\left[\frac{\partial\tilde{T}_{21}}{\partial y}+2\frac{\tilde{f}_2}{\tilde{a}_0}+\frac{\partial\tilde{T}_0}{\partial y}\right]_{y=0}=\mathscr{A}\dot{\tilde{f}}_2. \quad (45)$$

Similar equations can be derived for order ϵ^3 (Chahine & Liu 1983) and are not presented here for conciseness.

3.3. *Equivalence concept*

In order to have a physical insight into the phenomenon, it is interesting to find an equivalence between the behaviour of the bubble in the cloud and the simpler case of its behaviour under the action of another single bubble. As stated above, up to the order ϵ^2, the contribution of the cloud to the boundary condition at infinity for the test bubble is a superposition of a uniform pressure correction on the far-field pressure, $P_\infty(t)$, and of a uniform velocity field on the velocity, $V_\infty=0$. Both effects are compounded from single-bubble contributions. The uniform pressures are simply added while the velocities are compounded as vectors. These vectors are each of direction B^iB^j and of magnitude $\tilde{q}^j(l_0/l^{ij})^2$. Therefore, the $N-1$ bubbles other than $B^{(i)}$ can be replaced by a fictitious equivalent bubble having a strength $\tilde{q}^{ig}$, located at G^i, a distance l^{ig} from B^i in the direction defined by the angle $MB^iG^i=\theta^{ij}$. As

this equivalent bubble should induce the same pressures and velocities as defined by (34), its characteristics are obtained by the equations

$$\frac{\tilde{q}_n^{ig}}{\tilde{R}_0^{ig}} = \sum_{j \neq i} \frac{\tilde{q}_n^{j}}{\tilde{R}_0^{ij}}, \tag{46}$$

$$e_{ig} \frac{\tilde{q}_n^{ig}}{(\tilde{R}_0^{ig})^2} = \sum_{j \neq i} e_{ij} \frac{\tilde{q}_n^{j}}{(\tilde{R}_0^{ij})^2}, \tag{47}$$

where e_{ig} and e_{ij} are respectively unit vectors of the directions B^iG^i and B^iB^j (figure 1), and n is the order of approximation. These equations define the angle θ^{ig}, and the direction in which $\tilde{d}^i(t)$ is measured ((38) and (40)).

4. Numerical resolution

4.1. *General solution*

The system of equations derived up to order ϵ^3 constitute a set of 14 equations for the 14 unknown components of $R^i(\theta, t)$, and $T^i(\theta, t)$ ((36) and (37)). By solving this system one determines completely the flow and temperature fields as well as the bubble motion and deformation. A numerical solution of these equations is feasible and could be performed using the same procedure as Dalle Donne & Ferranti (1975). Their study dealt with a single-bubble growth and thus solved only equations (12), (15), and (17). Here the same approach would have to be performed for all seven components of the bubble radius (up to ϵ^3).

Since the equations are not independent, the procedure would start by determining at a given time step the temperature at the lowest order of approximation (ϵ^0) and the corresponding radius approximation. Knowing this, one can compute the successive temperature corrections, and the successive radius corrections. At each time step an iteration process would be used to insure a good correspondence between the obtained temperature and radius values. Stepping in time of the computation could be obtained with a Runge–Kutta procedure which solves each differential equation yielding the bubble-radius values. The determination of the temperature field is more elaborate and requires a stepping both in time and in space. This latter involves writing a finite-difference scheme and replacing the integration field with a grid of mesh points. This general solution is not developed here; we considered instead the cases where large initial superheats make a thermal-boundary-layer approximation valid.

4.2. *Thermal-boundary-layer approximation*

If the distance δ in which the temperature rises from its value at the bubble wall to approximately the imposed ambient temperature T_∞ is small compared with the bubble radius R, an approximate solution can be obtained more easily than with the method described in the preceding paragraph. By considering heat diffusion in the liquid, spherical bubble growth rate and heat balance at the bubble–liquid interface, Plesset & Prosperetti (1977) estimate δ/R by

$$\frac{\delta}{R} \simeq \frac{DL\rho_v}{K(T_\infty - T_b)} = \frac{\rho_v}{\rho} \frac{L}{C(T_\infty - T_b)} = J^{-1}. \tag{48}$$

Thus a boundary-layer approximation is valid as long as the Jacob number J is much larger than one. For a spherical bubble, comparisons between numerical computations

obtained using this approximation and those obtained by solving the exact equations gave very close agreement for $J \geqslant 3$ (Prosperetti & Plesset 1978; Plesset 1980).

When the boundary-layer approximation is used, the system of heat equations presented above simplifies considerably. Indeed, in that case the temperature departs from T_∞ only in the liquid region close to the bubble–liquid interface, and the values of r which are of interest are close to $R(\theta, t)$. The variable y defined in (27) is then small compared to $\tilde{a}_0^3$, and we can write

$$y = \xi \tilde{y} \tilde{a}_0^3, \tag{49}$$

where $\tilde{y}$ and $\tilde{a}_0$ are of order 1, and ξ is a small parameter [$\xi = O(J^{-1})$]. The problem considered then contains two small parameters ϵ and ξ, and an asymptotic solution uniformly valid when both ϵ and ξ go to zero can be obtained when a relationship between the two parameters is defined through the use of the principle of least degeneracy (Darrozes 1971).

Considering the heat equation (28) one can determine the relation needed between ϵ and ξ to conserve the maximum number of terms in the leading orders of approximation. In order to prevent the order-ϵ^0 expansion (29) from degenerating when ξ goes to zero, the Péclet number has to be large enough to satisfy

$$P_e = O(\xi^{-2}), \tag{50}$$

in which case both terms of the equation are conserved. Similarly, to conserve the maximum terms at the following-order ϵ one needs to keep together the leading terms coming from the expansions in powers of ϵ and those from expansions in powers of ξ (e.g. in the expansions of η^4). This 'least degeneracy' is obtained when

$$\xi = O(\epsilon). \tag{51}$$

Using the relationships (50) and (51) between P_e, ξ, and ϵ, the expansions become straightforward.

The equations obtained at the first-order expansion in both parameters (orders ϵ^0 and ξ^0) are those for the case of an isolated bubble. A solution is readily available in that case and was derived by Plesset & Zwick (1952) and Forster & Zuber (1954) using Laplace-transform methods. The non-dimensional temperature at the bubble wall is given by:

$$\tilde{T}_0(\tilde{a}_0, \tilde{t}) = \tilde{T}_\infty - \left(\frac{D}{\pi \tau_0}\right)^{\frac{1}{2}} \frac{r_{b_0}}{K(T_\infty - T_b)} \int_0^t L(x)\, \rho_v(x)\, \frac{\tilde{a}_0^2(x)\, \dot{\tilde{a}}_0(x)}{\left[\int_x^t \tilde{a}_0^4(y)\, \mathrm{d}y\right]^{\frac{1}{2}}}\, \mathrm{d}x, \tag{52}$$

where, to be consistent with the assumptions made in deriving this solution, D and K are constant and evaluated at T_b while L and ρ_v are functions of time. The numerical procedure is greatly simplified now that an analytical expression for the temperature at the bubble wall is known. The finite-element method which would have been used in the general case is here replaced by a numerical computation of the integral equation (52). An iteration procedure is required to insure that the computed value of $\tilde{T}_0(\tilde{a}_0, \tilde{t})$ does not differ significantly from the value presumed in the computation of the integrand.

Plesset & Zwick (1952) also gave the solution of the problem when (52) contains a right-hand side which is a known function of time (heat-source term). Using a matched asymptotic procedure they also computed the following order of approxi-

N Number of bubbles	c_1 $\Sigma\,\lambda_{ij}$	c_2 $\Sigma\,\dfrac{(\lambda_{ij})^2\cos\theta^{ij}}{\cos\theta^{ig}}$	c_3 $\Sigma\,(\lambda_{ij})^3\dfrac{3\cos^2\theta^{ij}-1}{3\cos^2\theta^{ig}-1}$
1	0	0	0
2	1	1	1
3	2	1.732	1.25
5	3	2	1
12	8.616	4.53	0.41

TABLE 1. Values of the numerical constants used in the computations

mation $O(\xi)$. These solutions correspond to the following-orders equations in powers of ϵ and ξ for the multi-bubble problem. For simplicity these equations will not be listed here.

5. Numerical illustration of the method

5.1. *Particular cases studied*

In order to illustrate the method presented above we consider numerical solutions for a cloud of simple geometry. The bubbles are distributed in a symmetrical configuration and are initially of equal size. With this configuration all bubbles have the same radius history, and the computation time is significantly reduced since no repeated computations for the various bubbles are needed. The computation is further simplified by the fact that all summations in the dynamic equations (24), (39), and (40) reduce to multiplications of the characteristics of a single bubble by one of the following three constants which depend only on the initial geometrical configuration of the cloud:

$$\left.\begin{aligned} c_1 &= \sum_{i\neq j}\lambda_{ij},\\ c_2 &= \sum_{i\neq j}(\lambda_{ij})^2\frac{\cos\theta^{ij}}{\cos\theta^{ig}},\\ c_3 &= \sum_{i\neq j}(\lambda_{ij})^3\frac{3\cos^2\theta^{ij}-1}{3\cos^2\theta^{ig}-1}. \end{aligned}\right\} \tag{53}$$

The values of c_1, c_2 and c_3 for the numerical computation presented below are listed in table 1.

An additional simplification of the numerical solution can be introduced if one notices that during the bubble growth the departure from the initial spherical shape happens very late in the bubble history and only when the asymptotic approach starts losing its validity. This is not true for the cloud collapse (Chahine 1982). Figure 2 shows the variation with time of the major radius of an individual bubble in a cloud configuration of N bubbles symmetrically located on a sphere. For this figure, heat transfer has been neglected. We observe, for the isolated bubble, the well-known asymptotic linear growth behaviour. However, when the number of interacting bubbles increases, the pressure field associated with the dynamics of the other bubbles in the cloud reduces the growth rate of the test bubble. This deviation increases with

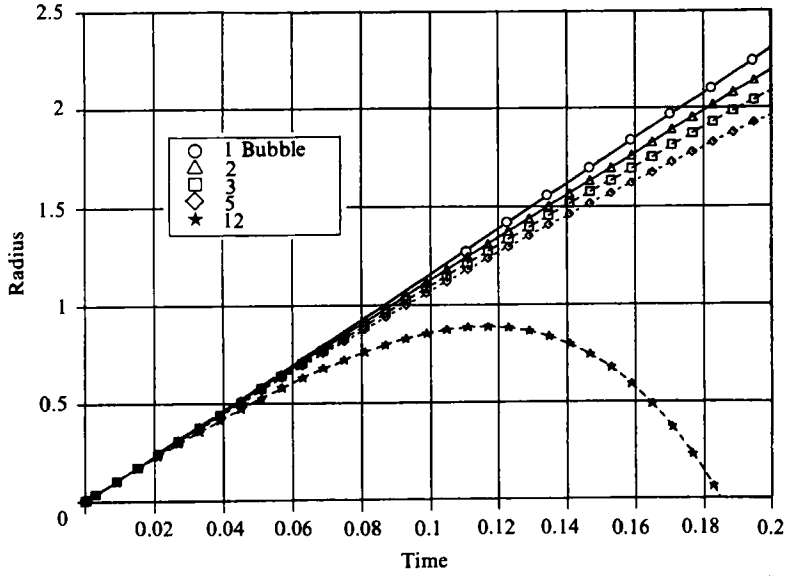

FIGURE 2. Growth of an initially spherical bubble in an N-bubble cloud following a sudden pressure drop, $W_e = 100$, $R_0 = 0.0001$ m, $\epsilon = 0.1$.

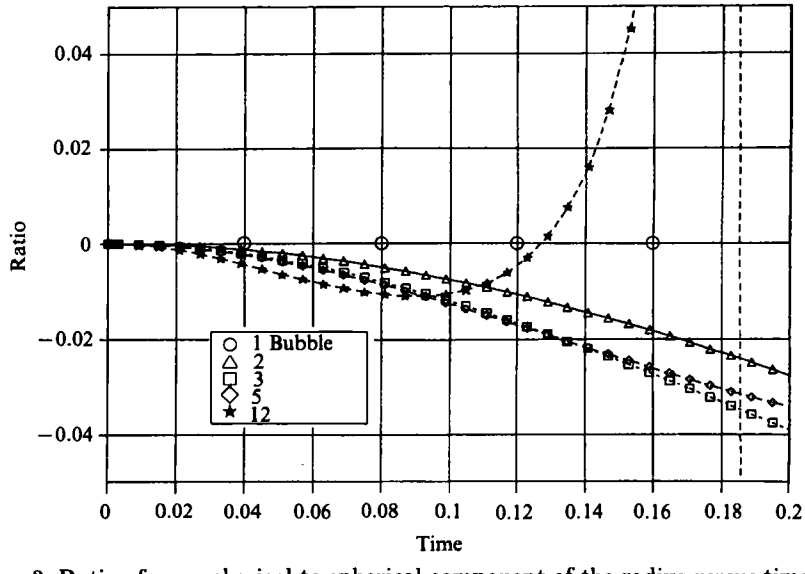

FIGURE 3. Ratio of non-spherical to spherical component of the radius *versus* time for a bubble growing in an N-bubble cloud. $W_e = 100$, $R_0 = 0.0001$ m, $\epsilon = 0.1$.

the number of bubbles N until, for $N = 12$ for the case studied, the method apparently fails for $t > 0.1$. The radius corrections (illustrated in the figure by the amount of deviation of the radius in an N-bubble case from the isolated-bubble case) become large compared with the order-zero radius. Figure 3 shows, for the same bubble configuration, the ratio of the non-spherical to the spherical part of $R(\theta, t)$ in the expansion (36). In all cases but the obvious one where the method breaks down, the relative deformations remain less than 4% while the bubble radius is 2000 times its initial value.

Based on this observation and as a first step towards a more precise solution, we have neglected in the developed numerical program the contribution of non-sphericity to the heat-transfer problem. Therefore, the temperature field was approximated by a spherically symmetrical field. However, this field accounts for interactions and differs from that of the isolated-bubble case because of the contributions of the higher-order spherical terms of the bubble equation. Indeed (52), relating the bubble-wall temperature to a spherical-bubble-radius history, was applied to the spherical part of the bubble radius, i.e. to

$$\bar{A}(t) = \tilde{a}_0(t) + \epsilon\tilde{a}_1(t) + \epsilon^2\tilde{a}_2(t) + \epsilon^3\tilde{a}_3. \tag{54}$$

With this simplification, at any time step all dynamical equations are solved using the value of the vapour pressure corresponding to the liquid temperature at the radial distance $\bar{A}(t)$. This temperature is computed at the preceding time step using (52). The non-spherical part of the bubble shape is not disregarded and is computed neglecting variations of the liquid temperature along the bubble surface. This is valid as long as the bubble deformation is negligible. Since we restrict this study to that case, the validity of the results is checked by monitoring the relative value of the computed non-spherical to the spherical components of the bubble-surface equation. The computation is stopped when an imposed limit is exceeded. Accounting for the deformations is an important task which we will consider in the continuation of this study.

5.2. *Results and interpretation*

A series of numerical cases was studied using a VAX 11/750 computer. We have considered different variations of the number of bubbles and configuration, the ambient pressures, the initial bubble radius, and the amount of superheat. The duration of a typical run was about 10 minutes of CPU time (for 2000 time steps). The computation involves the resolution of the heat and dynamical equations for an N-bubble configuration, the study of the corresponding case of an isolated bubble with and without heat transfer, and the computation of pressure histories at three locations in the flow field.

Figures 4–13 illustrate the results obtained on the influence of bubble interactions on the growth of a bubble in a superheated liquid that we will discuss below. In all figures, the curves are stopped when the computations become invalid owing to large bubble interactions. Figure 4 shows clearly the influence of interactions on the bubble-radius history. Since the bubble does not remain spherical, the value of $R(\theta^{ig})$ represented in this figure corresponds to the point on the bubble closest to the cloud centre, the 'lower-minor radius' (see figure 1). The classical results of asymptotic growth in t for the inertia-controlled bubble expansion and in t^{α} for the heat-controlled bubble expansion can be seen. If there was no pressure drop α would be $\frac{1}{2}$. However, here α is much closer to 1, as obtained by earlier studies on single bubbles (Jones & Zuber 1978; Theofanous *et al.* 1969; Cha & Henry 1981). The most important result obtained here is that bubble growth is inhibited by bubble interactions. Very clearly at a given time the bubble size decreases with the number of interacting bubbles. This decrease exceeds 20 % for a 5-bubble system for non-dimensional times larger than 10, or one millisecond after the start of the growth (see figure 4).

Figure 5 shows the effect of bubble interactions on the liquid temperature at the bubble wall. The presence of other growing bubbles in the field is seen to reduce the heat transfer at the bubble wall and thus the temperature drop in its vicinity. For example, for a 5-bubble system the deviation from the isolated-bubble case of the temperature drop is more than 30° one millisecond after the initial pressure drop. This

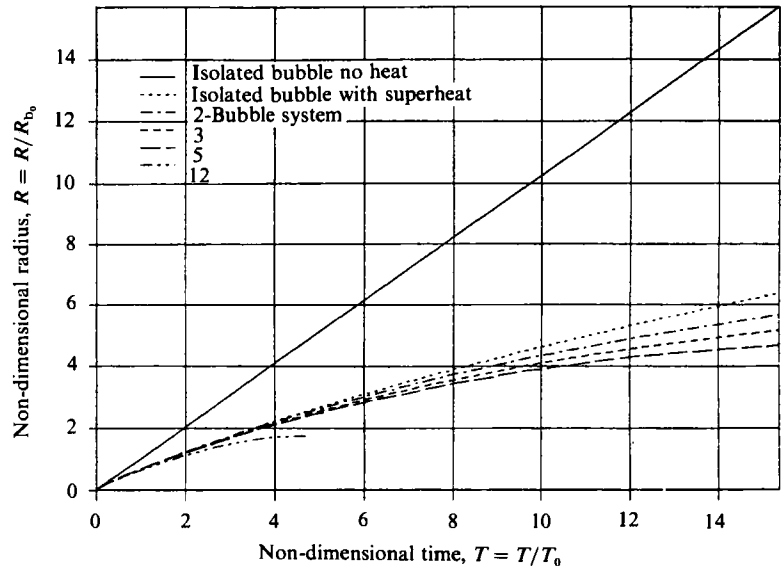

FIGURE 4. Influence of interactions on bubble growth in a superheated-liquid. Bubble-radius history, $P_0 = 2$ atm, $P_{inf} = 0.5$ atm, $\epsilon = 0.05$, $R_{b_0} = 0.01$ m, $R_0 = 2.5 \times 10^{-5}$ m, $T_b = 809.3$ °C, $T_{inf} = 1177.71$ °C, liquid sodium.

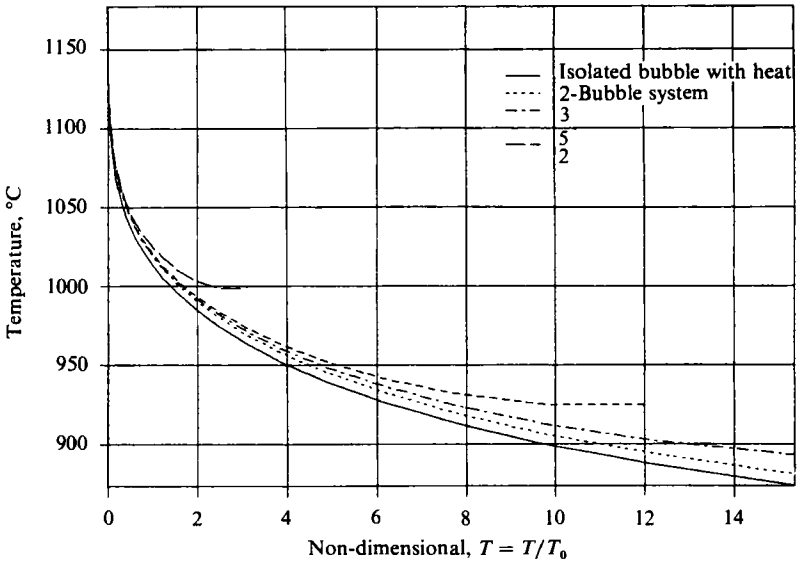

FIGURE 5. Influence of interactions on the temperature variations at the wall of a bubble in an N-bubble cloud, $P_0 = 2$ atm, $P_{inf} = 0.5$ atm, $\epsilon = 0.05$, $R_{b_0} = 0.01$ m, $R_0 = 2.5 \times 10^{-5}$ m, $T_b = 809.3$ °C, $T_{inf} = 1177.7$ °C, liquid sodium.

result, coupled with that obtained for the variations of the bubble radius, is important for any practical computation of heat transfer in a two-phase medium.

Figure 6 shows the modification of the bubble shape during its growth for the same N-bubble systems shown in figures 4 and 5. The bubble shapes at two instants during the growth process are represented. As expected, in the presence of an N-bubble cloud,

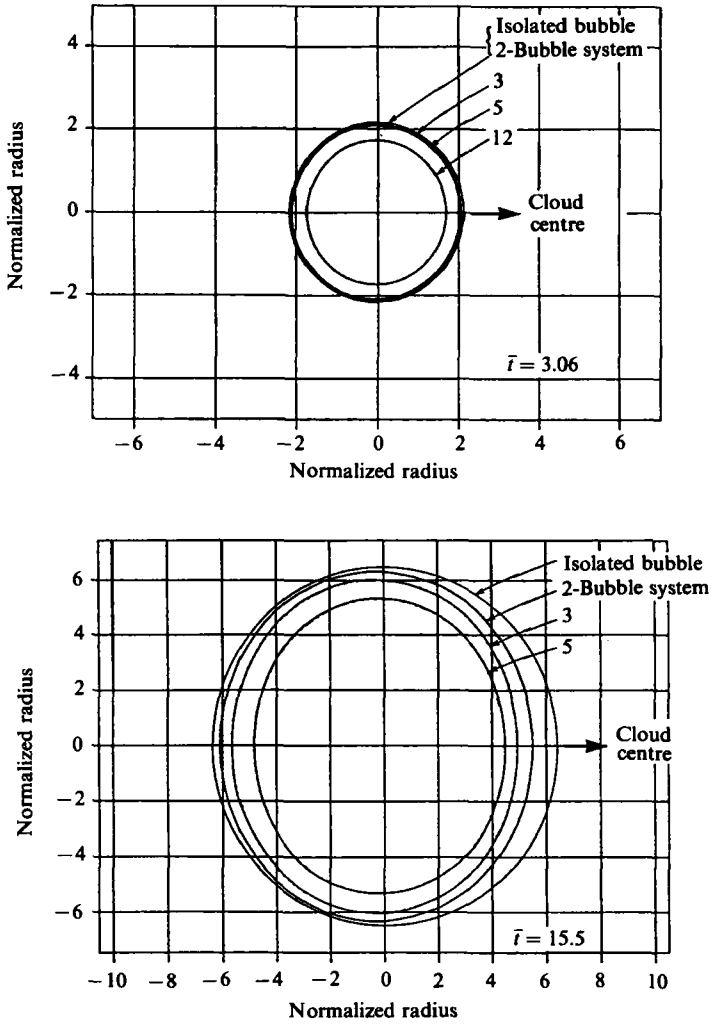

FIGURE 6. Variation with time of bubble shape characteristics at two selected times, $P_0 = 2$ atm, $P_{inf} = 0.5$ atm, $\epsilon = 0.05$, $R_{b_0} = 0.01$ m, $R_0 = 2.5 \times 10^{-5}$ m, $T_b = 809.3$ °C, $T_{inf} = 1177.71$ °C, liquid sodium.

the side of the bubble facing the cloud centre is seen to be slightly 'pushed away' from the cloud centre and the bubble is seen to elongate in a direction tangential to the sphere. However, any point on its surface always remains inside the corresponding fictitious isolated bubble growing under the same conditions. The deformation decreases as the number of interacting bubbles increases.

Figures 7 and 8 show the influence of the amount of pressure drop and initial superheat on the bubble growth. These figures consider an isolated bubble as well as a 5-bubble system. The same remarks made in the preceding paragraphs apply here when the influence of the number of bubbles is considered. In all cases the initial bubble radius is the same, and the pressure drops to the same value. However, since the initial pressures vary from one case to another and since all bubbles are considered to be initially at equilibrium, the initial temperature and thus the initial amount of superheat varies from one case to another. To isolate the two effects one has to

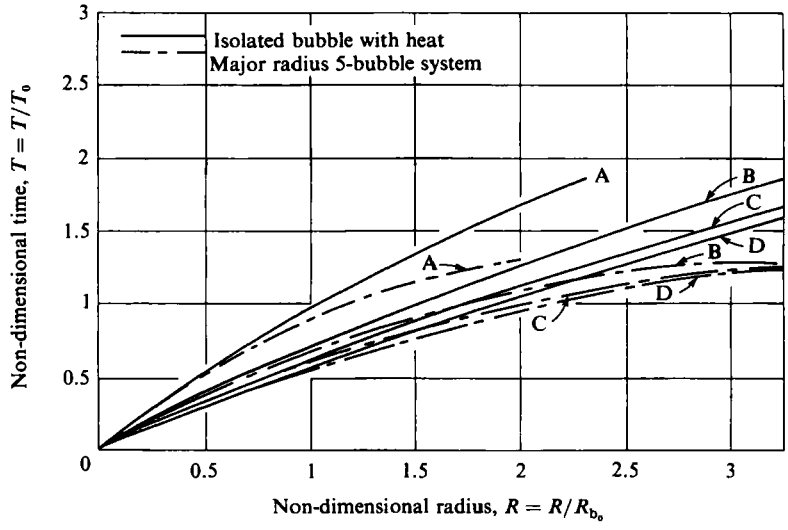

FIGURE 7. Influence of interactions and initial conditions on bubble growth in a superheated liquid, $P_{inf} = 1$ atm, $\epsilon = 0.4$, $R_{b_0} = 0.01$ m, $R_0 = 2.5 \times 10^{-5}$ m, $T_b = 879.9$ °C: A, $P_0 = 5$ atm, $T_{inf} = 1224.9$ °C; B, 3 atm, 1194.9 °C; C, 2 atm, 1177.7 °C; D, 1 atm, 1159.9 °C.

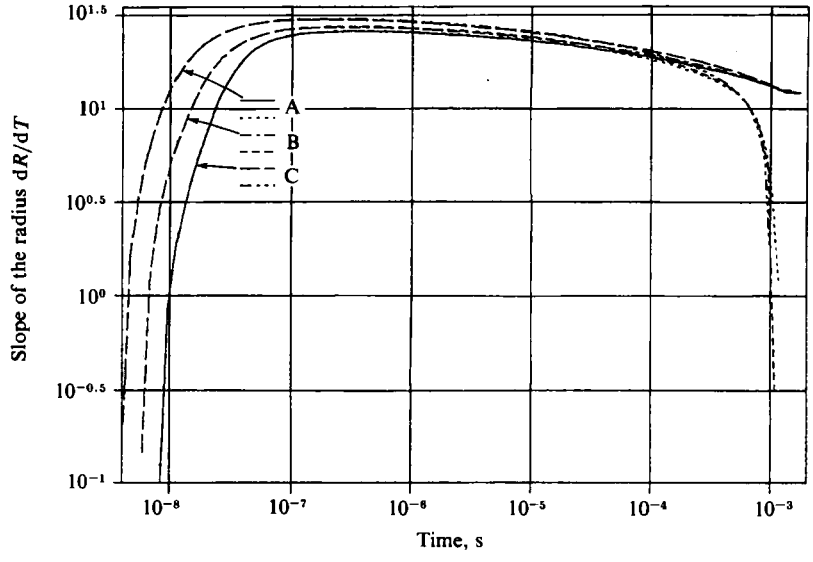

FIGURE 8. Influence of interactions and initial conditions on bubble growth rate in a superheated liquid, $P_{inf} = 1$ atm, $\epsilon = 0.4$, $R_{b_0} = 0.01$ m, $R_0 = 2.5 \times 10^{-5}$ m, $T_b = 879.9$ °C: A, $P_0 = 2$ atm, $T_{inf} = 1177.7$ °C; B, 3 atm, 1194.4 °C; C, 5 atm, 1224.9 °C.

consider the case where the bubbles are not initially at equilibrium. Another option would be to have the same initial pressure, radius and temperature and to vary the value of P_{inf}. We consider this case below. Figures 7 and 8 show that the normalized bubble radii and growth rates are larger at any given time when the amounts of pressure drop and superheat are greater. In the absence of heat transfer, scaling effects are mainly due to the differences in the Weber number W_e and the initial pressure parameter $\mathscr{P}$. When heat-transfer effects are included, there is an additional

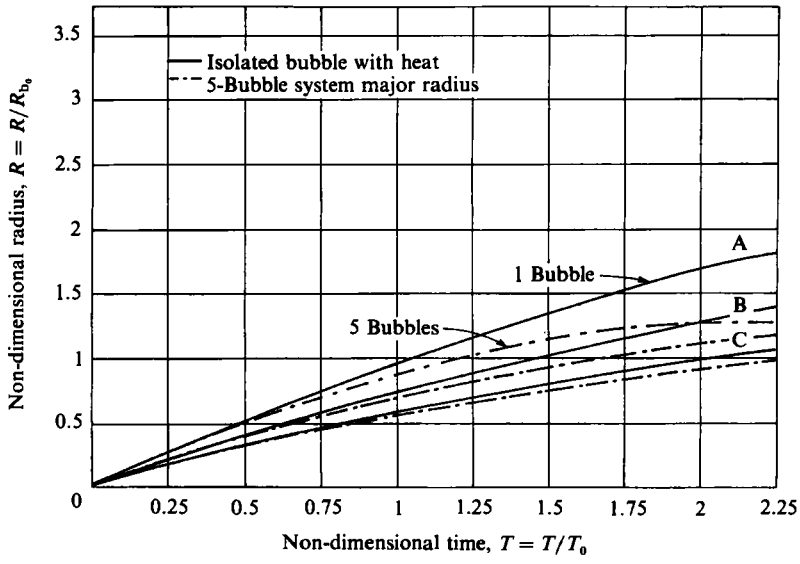

FIGURE 9. Influence of the imposed pressure P_{inf} on bubble growth in a superheated liquid, $P_0 = 5$ atm, $R_{b_0} = 0.01$ m, $R_0 = 2.5 \times 10^{-5}$ m, $\epsilon = 0.4$, $T_{inf} = 1224.9$ °C: A, $T_b = 879.9$ °C, $P_{inf} = 1$ atm; B, 960.5 °C, 2 atm; C, 1013.3 °C, 3 atm.

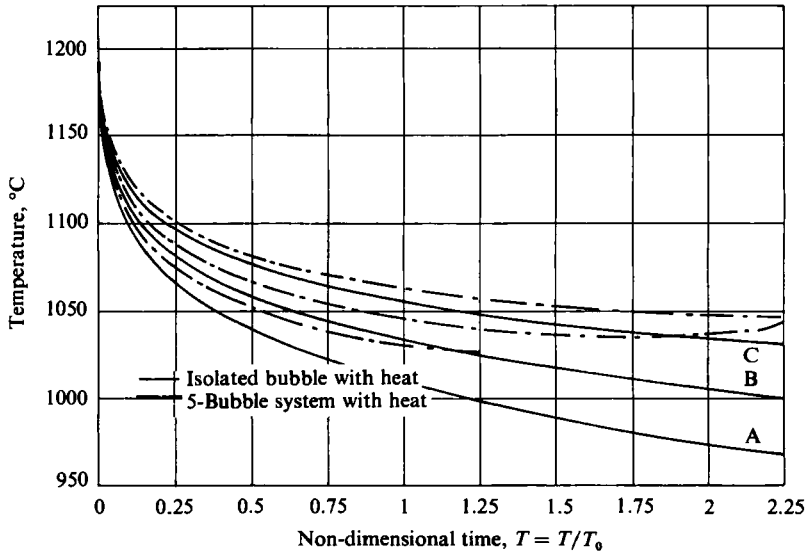

FIGURE 10. Influence of imposed pressure P_{inf} on the bubble-wall temperature, $P_0 = 5$ atm, $R_{b_0} = 0.01$ m, $R_0 = 2.5 \times 10^{-5}$ m, $\epsilon = 0.4$, $T_{inf} = 1224.9$ °C: A, $T_b = 879.9$ °C, $P_{inf} = 1$ atm; B, 960.5 °C, 2 atm; C, 1013.3 °C, 3 atm.

parameter, the Jacob number. These effects counterbalance each other in real time, and one observes a minor influence of the initial value of the pressure (for the same initial radius) when the radius variations are plotted with dimensional variables (Chahine & Liu 1983).

A similar result is seen when, for the same initial bubble radius and liquid temperature, the ambient pressure drops from the same initial pressure to different

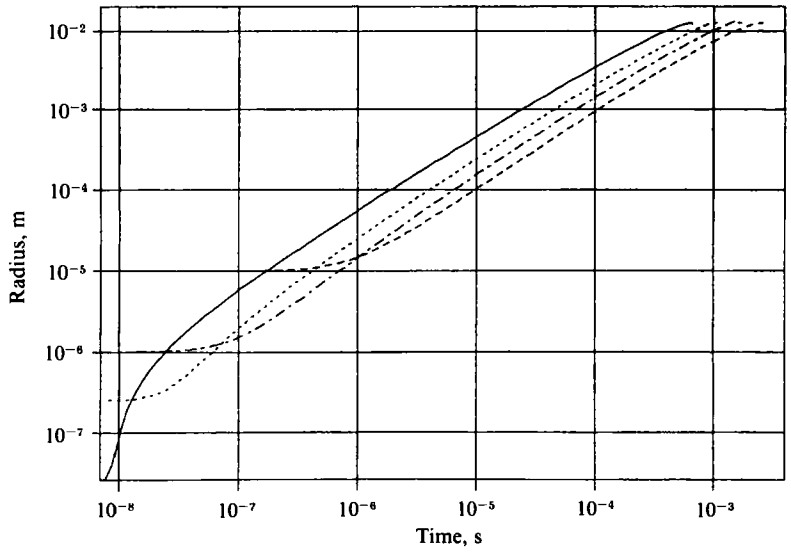

FIGURE 11. Influence of initial bubble size on radius history, $P_0 = 2$ atm, $P_{inf} = 1$ atm, $\epsilon = 0.2$, $R_{b_0} = 0.01$ m, $T_b = 879.9$ °C, 5-bubble system with superheat: ——, $R_0 = 2.5\text{E}-6$; ----, 2.5E−5; —·—, 1.0E−4; – – –, 1.0E−3.

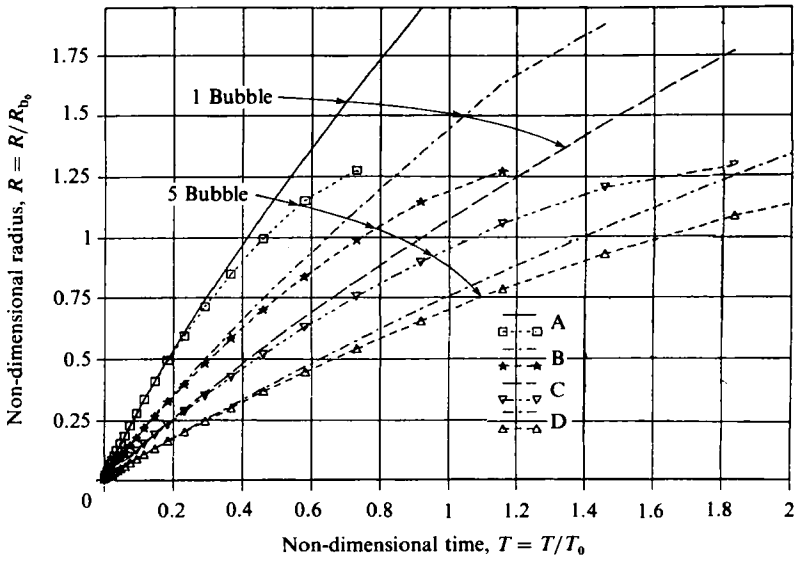

FIGURE 12. Influence of initial bubble size and bubble interactions on radius history, $P_0 = 2$ atm, $P_{inf} = 1$ atm, $\epsilon = 0.2$, $R_{b_0} = 0.01$ m, $T_b = 879.9$ °C: A, $T_{inf} = 1518.0$ °C, $R_0 = 2.5\text{E}-6$; B, 1177.7 °C, 2.5E−5; C, 1051.4 °C, 1.0E−4; D, 973.2 °C, 1.0E−3.

subsequent values. In this case the initial amount of superheat is the same for all the cases of pressure drop studied. However, the subsequent amounts of superheat differ from one case to another. The use of non-dimensional variables decreases (but does not cancel, because of nonlinearities) the influence of dynamic factors, but it does not alter thermal effects. The results (figure 9) show again a larger bubble radius

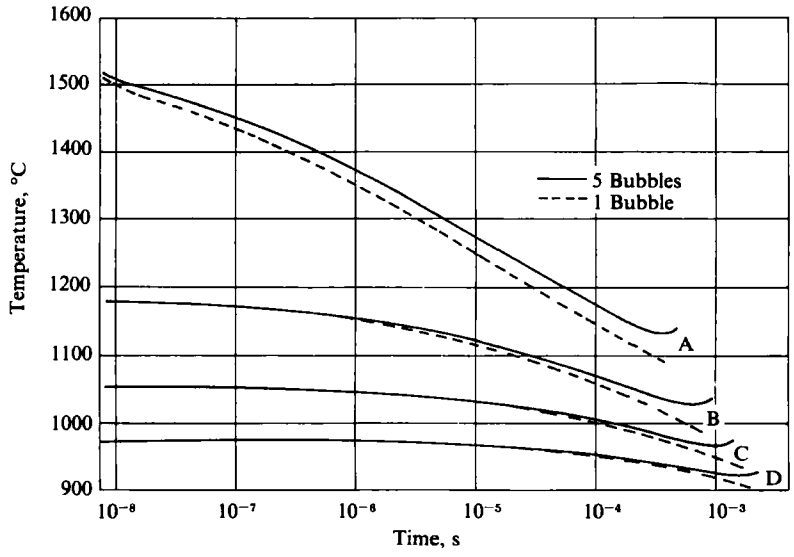

FIGURE 13. Influence of initial bubble size on bubble-wall-temperature history, $P_0 = 2$ atm, $P_{inf} = 1$ atm, $\epsilon = 0.2$, $R_{b_0} = 0.01$ m, $T_b = 879.9$ °C: A, $R_0 = 2.5\text{E}-6$; B, $2.5\text{E}-5$; C, $1.0\text{E}-4$; D, $1.0\text{E}-3$.

during the growth period for higher pressure drops. The comparison with the 5-bubble case can also be observed and shows again the retarding effect on bubble growth due to collective bubble behaviour. Figure 10 completes the picture by showing the temperature drop at the bubble wall for the different cases studied. The same observations as those made above are repeated, namely higher temperature drops for smaller pressure drops or higher number of interacting bubbles.

The last series of results elucidate the influence of the initial bubble size for given fixed pressure conditions. With the assumption that the bubble is initially at equilibrium, the modification of the initial bubble size also corresponds to a change of the amount of superheat. Figure 11 shows the predominance of the effect of the amount of superheat factor on the bubble growth; initially smaller bubbles attain greater sizes because of larger amounts of superheat. This effect is, however, coupled with the nonlinearities of the dynamical equations which favour smaller initial bubble radii in the first phase of the growth. Figure 12 shows the same effect with non-dimensional variables and compares a 5-bubble system with the isolated-bubble case. One can notice that the inhibition effect due to bubble interactions is larger for smaller initial bubbles or larger amounts of superheat. Finally, figure 13 describes the temperature drop at the bubble wall for the same cases.

6. Concluding remarks

We have developed in this study a theory for the growth of a cloud of bubbles in a superheated liquid. To do so we have used the method of matched asymptotic expansions assuming a low void fraction (small ratio of bubble radius to interbubble distance). Numerical solutions were then obtained for symmetrical cloud configurations using a multi Runge–Kutta scheme to solve the dynamical equations and a thin-thermal-boundary integral solution for the energy equations. The results

obtained show that bubble interactions significantly influence bubble growth and heat transfer. The effects of this influence can be summarized as follows:

(*a*) the growth rate of the bubble is reduced;

(*b*) the radius of any bubble at a given time is smaller than would be found for an isolated bubble; and

(*c*) the temperature drop at the bubble wall is smaller at any given time than would be found for an isolated bubble.

These effects increase with the number of interacting bubbles as well as with the amount of superheat and pressure drop. These results, which were obtained using small-perturbation assumptions, are expected to remain valid and become more significant when the void fraction becomes larger. Accounting for these effects is important for increasing the accuracies of the existing transient two-phase flow codes.

The study presented here could be improved by introducing a finite-speed wave propagation in the cloud and by accounting for the compressibility of the medium. The analytical equations derived for the general-bubble-configuration case (no symmetry or equal bubble size) could be expanded to a numerical approach in a relatively simple manner. The resolution of the problem could also be extended to low-superheat cases (small Jacob numbers) and to larger interactions and bubble deformations by numerically implementing the analytical approach presented above which was not used in the numerical examples.

This work was partially supported by the Naval Sea Systems Command, General Hydrodynamics Program administered by the David Taylor Naval Ship Research and Development Center under Contract Number N00014-82-C-009 and by a National Science Foundation Grant Number MEA-82606.89.

REFERENCES

BAUMEISTER, K. J. & HAMILL, T. D. 1969 Hyperbolic heat conduction equation – a solution for the semi-infinite body problem. *Trans. ASME* C: *J. Heat Transfer* **91**, 543–548.

CHA, Y. S. & HENRY, R. E. 1981 Bubble growth during decompression of a liquid. *Trans. ASME* C: *J. Heat Transfer* **103**, 56–60.

CHAHINE, G. L. 1981*a* Asymptotic theory of collective bubble growth and collapse. In *Proc. 5th Int. Symp. on Water Column Separation, IAHR, Obernach, Germany, September.*

CHAHINE, G. L. 1981*b* Experimental and asymptotic study of nonspherical bubble collapse. In *Proc. IUTAM Symp. on the Mechanics of Bubbles in Fluids, Pasadena, California,* also *Appl. Sci. Res.* **38**, 187–197, 1982.

CHAHINE, G. L. 1982 Cloud cavitation theory. *14th Symp. on Naval Hydrodynamics, Ann Arbor, Michigan, August,* pp. 165–195. Washington, D.C.: National Academy Press.

CHAHINE, G. L. & BOVIS, A. G. 1983 Pressure field generated by nonspherical bubble collapse. *Trans. ASME* I: *J. Fluids Engng* **105**, 356–364.

CHAHINE, G. L. & LIU, H. L. 1983 A singular perturbation theory of the growth of a bubble cluster in a superheated liquid. *Tracor Hydronautics Tech. Rep.* 83020-1.

DALLE DONNE, M. & FERRANTI, M. P. 1975 The growth of vapor bubbles in superheated sodium. *Intl J. Heat Mass Transfer* **18**, 477–493.

DARROZES, J. S. 1971 The method of matched asymptotic expansions applied to problems involving two singular perturbation parameters. *Fluid Dyn. Trans.* **6**, 119–129.

FORSTER, H. K. & ZUBER, N. 1954 Growth of a vapor bubble in a superheated liquid. *J. Appl. Phys.* **25**, 474–478.

HAMMITT, F. G. 1980 *Cavitation and Multiphase Flow Phenomena.* McGraw-Hill.

JONES, O. C. & ZUBER, N. 1978 Bubble growth in variable pressure fields. *Trans. ASME* C: *J. Heat Transfer* **100**, 453–459.

MORCH, K. A. 1981 Energy considerations on the collapse of cavity clusters. *Proc. IUTAM Symp. on the Mechanics of Bubbles in Fluids, Pasadena, California.*

PLESSET, M. S. 1980 New problems in two-phase flows. In *Proc. 10th IAHR Symp. on Hydraulic Machinery and Equipment Associated With Energy Systems in the New Decade of the 1980's, Tokyo, October*, pp. 31–40.

PLESSET, M. S. & PROSPERETTI, A. 1977 Bubble dynamics and cavitation. *Ann. Rev. Fluid Mech.* **9**, 145–185.

PLESSET, M. S. & ZWICK, S. A. 1952 A nonsteady heat diffusion problem with spherical symmetry. *J. Appl. Phys.* **23**, 95–98.

PROSPERETTI, A. & PLESSET, M. S. 1978 Vapor-bubble growth in a superheated liquid. *J. Fluid Mech.* **85**, 349–368.

THEOFANOUS, T., BIASI, L., ISBIN, H. S. & FAUSKE, H. 1969 A theoretical study of bubble growth in constant and time dependent pressure fields. *Chem. Engng Sci.* **24**, 885–897.

VAN DYKE, M. 1964 *Perturbation Methods in Fluid Mechanics.* Academic.